

APPLICATION OF EVOLUTIONARY ALGORITHMS FOR IDENTIFICATION OF DUAL PHASE LAG MODEL PARAMETERS

Bohdan Mochnacki¹, Marek Paruch²

¹ *Institute of Mathematics, Czestochowa University of Technology, Poland*

² *Department of Strength of Materials and Computational Mechanics*

Silesian University of Technology, Poland

bohdan.mochancki@im.pcz.pl, marek.paruch@polsl.pl

Abstract. The dual phase lag model (DPLM) based on the generalized form of Fourier law, in particular the introduction of two ‘delay times’ (relaxation time τ_q and thermalization time τ_T) leads to the considered form of energy equation. This equation should be applied in the case of microscale heat transfer modeling. In particular, DPLM constitutes a good approximation of thermal processes which are characterized by extremely short duration (e.g. ultrafast laser pulse), extreme temperature gradients and geometrical features of the domain considered (e.g. thin metal film). In this paper, the identification problem of two of the above mentioned positive constants τ_q, τ_T is discussed and the thermal processes proceeding in the domain of thin metal film subjected to a laser beam are analyzed. At the stage of computations connected with the identification problem solution, evolutionary algorithms are used. To solve the problem, additional information concerning the transient temperature distribution on a metal film surface is assumed to be known.

Introduction

Let us consider the following form of generalized Fourier law

$$\mathbf{q}(x, t + \tau_q) = -\lambda \nabla T(x, t + \tau_T) \quad (1)$$

where \mathbf{q} is the unitary heat flux, λ is the thermal conductivity, ∇T is the temperature gradient, τ_q, τ_T correspond to the relaxation time, which is the mean time for electrons to change their energy states and the thermalization time, which is the mean time required for electrons and lattice to reach equilibrium.

The DPLM equation can be, among others, reduced from the considerations concerning the parabolic two-temperature model [1-3]. This model involves two energy equations determining the heat transfer in the electron gas and metal lattice. The equations creating the model discussed (in the case of metals) are of the form

$$c_e(T_e) \frac{\partial T_e}{\partial t} = \nabla[\lambda_e(T_e) \nabla T_e] - G(T_e - T_l) \quad (2)$$

$$c_l(T_l) \frac{\partial T_l}{\partial t} = G(T_e - T_l), \quad (3)$$

where $T_e = T_e(x, t)$, $T_l = T_l(x, t)$ are the temperatures of the electrons and lattice, respectively, $c_e(T_e)$, $c_l(T_l)$ are the volumetric specific heats, $\lambda_e(T_e)$, $\lambda_l(T_l)$ are the thermal conductivities, G is the coupling factor [1], which characterizes the energy exchange between phonons and electrons [4]. Equations (1), (2) under the assumption that volumetric specific heats c_e and c_l are constant values, using a certain elimination technique can be substituted by a single equation containing a higher-order mixed derivative in both time and space. From equation (2) it results that

$$T_e = T_l + \frac{c_l}{G} \frac{\partial T_l}{\partial t} \quad (4)$$

Putting (3) into (1), one has

$$c_e \left(\frac{\partial T_l}{\partial t} + \frac{c_l}{G} \frac{\partial^2 T_l}{\partial t^2} \right) = \nabla(\lambda_e \nabla T_l) + \frac{c_l}{G} \nabla \left[\lambda_e \frac{\partial}{\partial t} (\nabla T_l) \right] - c_l \frac{\partial T_l}{\partial t} \quad (5)$$

this means

$$(c_e + c_l) \left[\frac{\partial T_l}{\partial t} + \frac{c_e c_l}{G(c_e + c_l)} \frac{\partial^2 T_l}{\partial t^2} \right] = \nabla(\lambda_e \nabla T_l) + \frac{c_l}{G} \frac{\partial}{\partial t} [\nabla \lambda_e (\nabla T_l)] \quad (6)$$

Denoting

$$\tau_r = \frac{c_l}{G}, \quad \tau_q = \frac{1}{G} \left(\frac{1}{c_e} + \frac{1}{c_l} \right)^{-1} \quad (7)$$

finally, one obtains

$$c \left[\frac{\partial T(x, t)}{\partial t} + \tau_q \frac{\partial^2 T(x, t)}{\partial t^2} \right] = \nabla[\lambda \nabla T(x, t)] + \tau_r \nabla \left[\lambda \frac{\partial \nabla T(x, t)}{\partial t} \right] \quad (8)$$

where $T(x, t) = T_l(x, t)$ is the macroscopic lattice temperature [5], $c = c_l + c_e$ is the effective volumetric specific heat resulting from the serial assembly of electrons and phonons and $\lambda = \lambda_e$ [6].

In Figure 1 (see [11]), the numerical solution obtained on the basis of two temperature parabolic models is shown (equations (2) and (3)). In particular, the heat-

ing/cooling curves refer to the surface of domain (Ti) subjected to a laser pulse. The time for which the electrons and lattice temperatures are equalized correspond to the thermalization one τ_T . Hence, it seems that the physical interpretation of this parameter is self-evident.

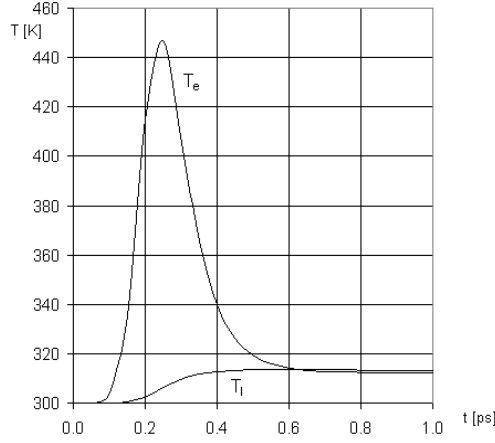


Fig. 1. Changes of surface temperatures

The other approach to DPLM formulation is also possible and the details of the mathematical considerations leading to the same equation can be found in [3].

1. Internal heat source

In this paper the thermal interactions between external heating (laser beam) and the domain of metal film are taken into account by the introduction of a additional term supplementing the DPLM, in particular the function corresponding to volumetric internal heat sources, $Q(x, t)$ is considered. This approach is often used [2] while the new form of energy equation in which $Q(x, t)$ appears is the following:

$$c \left[\frac{\partial T(x, t)}{\partial t} + \tau_q \frac{\partial^2 T(x, t)}{\partial t^2} \right] = \nabla [\lambda \nabla T(x, t)] + \tau_T \nabla \left[\lambda \frac{\partial \nabla T(x, t)}{\partial t} \right] + Q(x, t) + \tau_q \frac{\partial Q(x, t)}{\partial t} \quad (9)$$

The formula determining the capacity of internal heat sources is applied (1D problem [7, 8]) takes the form of

$$Q(x, t) = \sqrt{\frac{\mu}{\pi}} \frac{1-R}{t_p \delta} I_0 \exp \left[-\frac{x}{\delta} - \mu \frac{(t-2t_p)^2}{t_p^2} \right] \quad (10)$$

where I_0 is the laser intensity which is defined as the total energy carried by a laser pulse per unit cross-section of the laser beam, t_p is the characteristic time of a laser pulse, δ is the characteristic transparent length of irradiated phonons called the absorption depth and R is the surface reflectivity, $\mu = 4 \ln 2$. The local and temporary value of Q results from distance x between the surface subjected to laser action and the point considered. Using this approach, the no-flux boundary conditions for $x = 0$ and $x = L$ should be assumed.

In Figure 2, the metal film subjected to a laser beam is shown, at the same time, the geometrical features of the domain considered allows one to treat the problem as a 1D one.

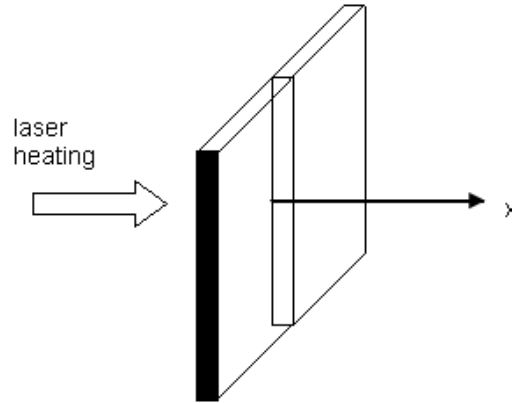


Fig. 2. Domain considered

2. Numerical solution based on FDM (direct problem)

At the stage of numerical modeling, the finite difference method in the version proposed by Mochnacki and Suchy [9] has been used. Therefore, the following basic energy equation (1D problem) is considered

$$c \left[\frac{\partial T(x,t)}{\partial t} + \tau_q \frac{\partial^2 T(x,t)}{\partial t^2} \right] = \frac{\partial}{\partial x} \left[\lambda \frac{\partial T(x,t)}{\partial x} \right] + \tau_r \frac{\partial}{\partial t} \frac{\partial}{\partial x} \left[\lambda \frac{\partial T(x,t)}{\partial x} \right] + Q(x,t) + \tau_q \frac{\partial Q(x,t)}{\partial t} \quad (11)$$

The differential mesh is created as a Cartesian product of spatial Δ_h and time Δ_t meshes. The time grid is defined as follows:

$$\Delta_t: t^0 < t^1 < \dots < t^{f-2} < t^{f-1} < t^f < \dots < t^F < \infty \quad (12)$$

while the spatial mesh is shown in Figure 3.

It is visible that the 'boundary' nodes are located at a distance of $0.5 h$ from the real boundaries (this type of discretization assures a very simple and exact approximation of boundary conditions [9]).

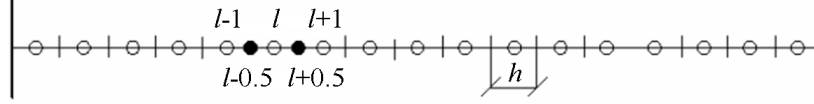


Fig. 3. Spatial mesh

The FDM approximation of the spatial differential operator can be taken as follows [9]:

$$\frac{\partial}{\partial x} \left(\lambda \frac{\partial T}{\partial x} \right)_i^f = \frac{T_{i+1}^f - T_i^f}{R_{i+1}^{f-1}} \Psi_{i+1} + \frac{T_{i-1}^f - T_i^f}{R_{i-1}^{f-1}} \Psi_{i-1} \quad (13)$$

where $\Psi_{i+1} = \Psi_{i-1} = 1/h$ are the mesh shape functions, while

$$R_{i+1}^{f-1} = \frac{0.5h}{\lambda_i^{f-1}} + \frac{0.5h}{\lambda_{i+1}^{f-1}}, \quad R_{i-1}^{f-1} = \frac{0.5h}{\lambda_i^{f-1}} + \frac{0.5h}{\lambda_{i-1}^{f-1}} \quad (14)$$

are the thermal resistances between node i and adjoining nodes $i+1$, $i-1$. Index f in formula (13) shows that the implicit differential scheme will be used here, at the same time, the thermal conductivities are taken for time t^{f-1} to obtain the linear form of final FDM equations. The FDM approximation of equation (11) for transition $t^{f-1} \rightarrow t^f$ is of the form

$$\begin{aligned} & c \frac{T_i^f - T_i^{f-1}}{\Delta t} + c \tau_q \frac{T_i^f - 2T_i^{f-1} + T_i^{f-2}}{(\Delta t)^2} = \\ & \frac{T_{i+1}^f - T_i^f}{R_{i+1}^{f-1}} \Psi_{i+1} + \frac{T_{i-1}^f - T_i^f}{R_{i-1}^{f-1}} \Psi_{i-1} + \frac{\tau_T}{\Delta t} \left(\frac{T_{i+1}^f - T_i^f}{R_{i+1}^{f-1}} \Psi_{i+1} + \frac{T_{i-1}^f - T_i^f}{R_{i-1}^{f-1}} \Psi_{i-1} \right) - \\ & \frac{\tau_T}{\Delta t} \left(\frac{T_{i+1}^{f-1} - T_i^{f-1}}{R_{i+1}^{f-1}} \Psi_{i+1} + \frac{T_{i-1}^{f-1} - T_i^{f-1}}{R_{i-1}^{f-1}} \Psi_{i-1} \right) + Q_i^f + \tau_q \left(\frac{\partial Q}{\partial t} \right)_i^f \end{aligned} \quad (15)$$

and the last formula can be written as follows

$$\begin{aligned} & A_i T_{i-1}^f + B_i T_i^f + C_i T_{i+1}^f = \\ & D_i T_{i-1}^{f-1} + E_i T_i^{f-1} + F_i T_{i+1}^{f-1} + \frac{\tau_q}{(\Delta t)^2} T_i^{f-2} - \\ & \frac{Q_i^f}{c} - \frac{\tau_q}{c} \left(\frac{\partial Q}{\partial t} \right)_i^f, \quad i = 1, 2, \dots, N \end{aligned} \quad (16)$$

where

$$A_i = \frac{\Psi_{i-1}}{c R_{i-1}^{f-1}} \left(1 + \frac{\tau_T}{\Delta t} \right), \quad C_i = \frac{\Psi_{i+1}}{c R_{i+1}^{f-1}} \left(1 + \frac{\tau_T}{\Delta t} \right) \quad (17)$$

$$B_i = -\frac{1}{\Delta t} \left(1 + \frac{\tau_q}{\Delta t} \right) - A_i - C_i \quad (18)$$

$$D_i = \frac{\Psi_{i-1}}{c R_{i-1}^{f-1}} \frac{\tau_T}{\Delta t}, \quad F_i = \frac{\Psi_{i+1}}{c R_{i+1}^{f-1}} \frac{\tau_T}{\Delta t} \quad (19)$$

$$E_i = -\frac{1}{\Delta t} \left(1 + \frac{2\tau_q}{\Delta t} \right) - D_i - F_i \quad (20)$$

Finally,

$$A_i T_{i-1}^f + B_i T_i^f + C_i T_{i+1}^f = G_i^f \quad (21)$$

where

$$G_i^f = D_i T_{i-1}^{f-1} + E_i T_i^{f-1} + F_i T_{i+1}^{f-1} + \frac{\tau_q}{(\Delta t)^2} T_i^{f-2} - \frac{Q_i^f}{c} - \frac{\tau_q}{c} \left(\frac{\partial Q}{\partial t} \right)_i^f \quad (22)$$

The same equations are accepted for the nodes close to the boundaries. It is enough to assume that the thermal resistances in directions 'to the boundary' are sufficiently big (e.g. 10^{10}) and then the non-flux condition is taken into account. The starting point of the numerical simulation process results from the initial conditions, in particular $T_i^0 = T_i^1 = T_0$, $i = 1, 2, \dots, N$. As was mentioned, the system of FDM equations (16) has been solved using the Thomas algorithm [9] for a three-diagonal linear system of algebraic equations.

3. Inverse problem

To solve the inverse problem, the least squares criterion is applied

$$S(\tau_q, \tau_T) = \frac{1}{MF} \sum_{i=1}^M \sum_{f=1}^F (T_i^f - T_{di}^f)^2 \quad (23)$$

where T_{di}^f and $T_i^f = T(x_i, t^f)$ are the measured and estimated temperatures, respectively and M is the number of sensors. The minimum of functional (23) has

been found using evolutionary algorithms. Hence, the direct problems have been solved and the results allow one to determine the time dependent surface temperature ($x = 0$). Because the temperature history resulting from the numerical solution for the basic input data is very close to the experimental ones quoted in [10] - Figure 4, therefore this undisturbed numerical solution is assumed to be a base of the identification problem solution ('measured surface temperature'). Therefore, the laser parameters determining the capacity of internal source function $Q(x, t)$ and also the thermal conductivity and volumetric specific heat of gold are known, parameters τ_q , τ_T should be determined (from the practical standpoint the experimental estimation of τ_q , τ_T is not easy).

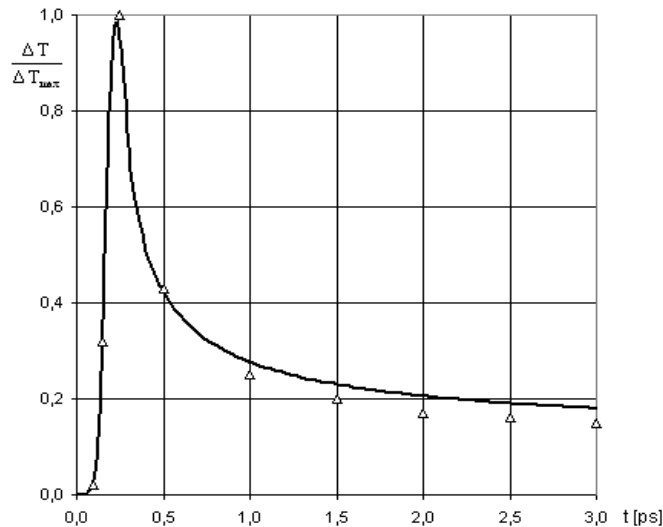


Fig. 4. Comparison to experimental data [10]

In Figures 5 and 6, an example of a direct problem solution is shown. The layer is subjected to a short-pulse laser irradiation whose parameters are equal to: $R = 0.93$ (reflectivity), $I_0 = 13.7 \text{ J/m}^2$ (intensity), $t_p = 0.1 \text{ ps} = 10^{-13} \text{ s}$ (time of laser pulse), $\delta = 15.3 \text{ nm}$ (absorption depth). The following parameters of thin gold film are assumed: thermal conductivity $\lambda = 317 \text{ W/(mK)}$, volumetric specific heat $c = 2.4897 \text{ MJ/(m}^3\text{K)}$, relaxation time $\tau_q = 8.5 \text{ ps}$, thermalization time $\tau_T = 90 \text{ ps}$. The initial temperature equals $T_0 = 20^\circ\text{C}$ (see [11-13]).

Using the algorithm presented in the previous chapter under the assumption that $N = 200$ and $\Delta t = 0.005 \text{ ps}$, the transient temperature field has been found. In Figure 5 the temperature profiles are shown, while Figure 6 illustrates the courses of heating (cooling) curves at points selected from the domain considered.

The identification of 'delay' times has been done using evolutionary algorithms. In Table 1 the algorithm parameters are collected. The results obtained are presented in Table 2 and they are quite satisfactory.

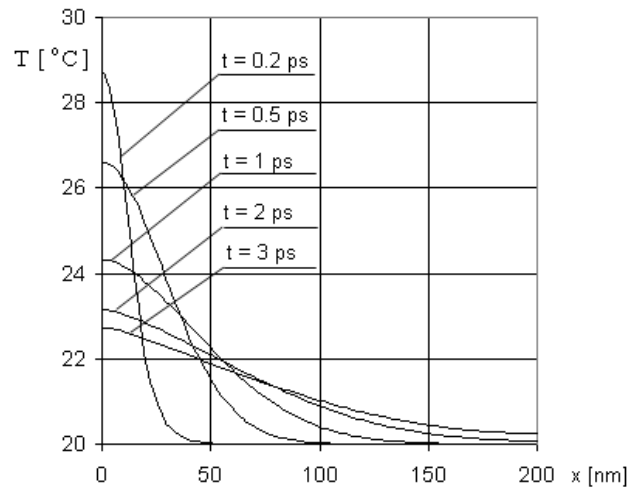


Fig. 5. Temperature profiles

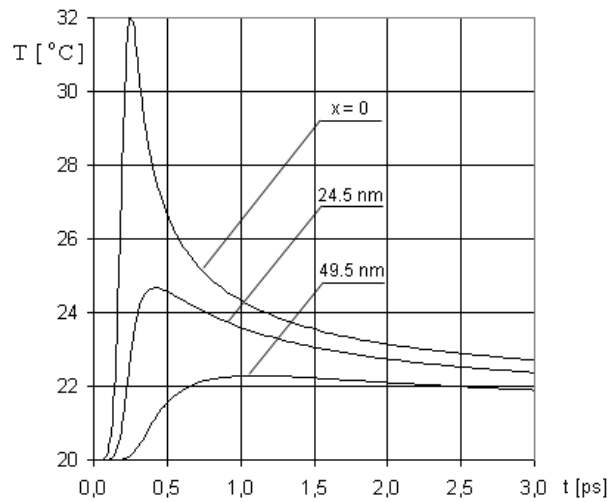


Fig. 6. Cooling (heating) curves

Table 1

Evolutionary algorithm parameters

No. of generations	Number of chromosomes	Prob. of uniform mutation	Prob. of non-uniform mutation	Prob. of arithmetic crossover	Prob. of cloning
50	20	20%	30%	50%	10%

Table 2

Result of computations using EA

Design variable	Exact value	Found value	Error, %
τ_q	$8.5 \cdot 10^{-12}$	$8.499999 \cdot 10^{-12}$	0
τ_r	$90 \cdot 10^{-12}$	$89.999999 \cdot 10^{-12}$	0

The application of evolutionary algorithms for the identification of problems solutions is (from the numerical point of view) a time-consuming one. On the other hand however, the mathematical and numerical problems connected with adequate algorithm construction seem to be essentially simpler in comparison to the very popular gradient methods.

Acknowledgement

The paper presented previously as a lecture during the conference Solidification and Crystallization of Metals, Kielce, 2011 was supported by Grant No N N501 2176 37 (Polish Ministry of Science and Higher Education).

References

- [1] Al-Nimr M.A., Heat transfer mechanisms during short duration laser heating of thin metal films, International Journal of Thermophysics 1997, 18, 5, 1257-1268.
- [2] Lin Z., Zhigilei L.V., Electron-phonon coupling and electron heat capacity of metals under conditions of strong electron-phonon nonequilibrium, Physical Review B 2008, 77, 075133-1-075133-17.
- [3] Majchrzak E., Mochnacki B., Greer A.L., Suchy J.S., CMES: Computer Modelling in Engineering & Sciences 2009, 41, 2, 131-146.
- [4] Tian W., Yang R., Phonon transport and thermal conductivity percolation in random nanoparticle composites, CMES: Computer Modeling in Engineering & Sciences 2008, 24, 2, 3, 123-142.
- [5] Ozisik M.N., Tzou D.Y., On the wave theory in heat conduction, Journal of Heat Transfer 1994, 116, 526-535.
- [6] Tzou D.Y., Chiu K.S., Temperature-dependent thermal lagging in ultrafast laser heating, Int. Journal of Heat and Mass Transfer 2001, 44, 1725-1734.
- [7] Kaba I.K., Dai W., A stable three-level finite difference scheme for solving the parabolic two-step model in a 3D micro-sphere heated by ultrashort-pulsed lasers, Journal of Computational and Applied Mathematics 2005, 181, 125-147.
- [8] Chen J.K., Beraun J.E., Numerical study of ultrashort laser pulse interactions with metal films, Numerical Heat Transfer, Part A 2001, 40, 1-20.
- [9] Mochnacki B., Suchy J.S., Numerical Methods in Computations of Foundry Processes, Polish Foundrymen's Technical Association, Cracow 1995.
- [10] Tang D.W., Araki N., Int. Journal of Heat and Mass Transfer 1999, 32, 855-860.

- [11] Majchrzak E., Poteralska J., Two temperature model of microscopic heat transfer, *Computer Method in Material Science* 2011, 11, 2, 337-342.
- [12] Majchrzak E., Poteralska J., Two-temperature microscale heat transfer model. Part 1: Determination of electrons parameters, *Scientific Research of the Institute of Mathematics and Computer Science* 2010, 1(9), 99-108.
- [13] Majchrzak E., Poteralska J., Two-temperature microscale heat transfer model. Part 2: Determination of lattice parameters, *Scientific Research of the Institute of Mathematics and Computer Science* 2010, 1(9), 109-120.